HAL
open science

The field high-amplitude SX Phoenicis variable BL Camelopardalis: results from a multisite photometric campaign. I. Pulsation

E. Rodríguez, S. Fauvaud, J. A. Farrell, A.-Y. Zhou, Jean-Pierre Sareyan, M. J. López-González, Marc-Antoine Dupret, A. Grigahcène, Joris de Ridder, G. Klingenberg, et al.

To cite this version:

E. Rodríguez, S. Fauvaud, J. A. Farrell, A.-Y. Zhou, Jean-Pierre Sareyan, et al.. The field high-amplitude SX Phoenicis variable BL Camelopardalis: results from a multisite photometric campaign. I. Pulsation. Astronomy and Astrophysics - A&A, 2007, 471, pp.255-264. 10.1051/0004-6361:20077514 . hal-03733398

HAL Id: hal-03733398

https://hal.science/hal-03733398v1

Submitted on 6 Oct 2022

HAL is a multi-disciplinary open access archive for the deposit and dissemination of scientific research documents, whether they are published or not. The documents may come from teaching and research institutions in France or abroad, or from public or private research centers.

L'archive ouverte pluridisciplinaire **HAL**, est destinée au dépôt et à la diffusion de documents scientifiques de niveau recherche, publiés ou non, émanant des établissements d'enseignement et de recherche français ou étrangers, des laboratoires publics ou privés.

A&A 471, 255–264 (2007)
DOI: 10.1051/0004-6361:20077514
© ESO 2007

Astronomy & Astrophysics

The field high-amplitude SX Phoenicis variable BL Camelopardalis: results from a multisite photometric campaign

I. Pulsation

E. Rodríguez[1], S. Fauvaud[2,3], J. A. Farrell[4], A.-Y. Zhou[5], J.-P. Sareyan[6], M. J. López-González[1], M.-A. Dupret[7], A. Grigahcéne[8], J. de Ridder[9], G. Klingenberg[10], M. Wolf[11], P. Van Cauteren[12], P. Lampens[13], D. Martínez[1], V. M. Casanova[1], F. J. Aceituno[1], M. Helvaci[14], E. G. Hintz[15], L. Král[16], F. Fumagalli[3], J. H. Simonetti[17], B. H. Granslo[10], L. Kotková[18], G. Santacana[2], J. Michelet[19], M. Fauvaud[2], J.-M. Vugnon[20], H. Sadsaoud[8], S. Aliouane[8], Z. C. Grigahcéne[8], S. Martín-Ruíz[1], P. J. Amado[1], J. C. Suárez[1], A. Moya[1], H. Kučáková[16], R. Kocián[16], K. Truparová[16], A. Avdibegović[11], M. Blažek[11], J. Kliner[11], P. Zasche[11], M. Vilásek[16], S. Bartošíková[16], B. Yasarsoy[21], C. Ulusoy[21], K. A. Graham[22], M. P. Nicholson[22], O. Trondal[10], C. Yesilyaprak[23], and D. Coker[14]

(Affiliations can be found after the references)

Received 20 March 2007 / Accepted 7 June 2007

ABSTRACT

Context. BL Cam is an extreme metal-deficient field high-amplitude SX Phe-type variable where a very complex frequency spectrum is detected, with a number of independent nonradial modes excited, unusual among the high-amplitude pulsators in the Lower Classical Instability Strip.
Aims. An extensive and detailed study has been carried out to investigate the pulsational content and properties of this object.
Methods. The analysis is based on 283 h of CCD observations obtained in the Johnson V filter, during a long multisite photometric campaign carried out along the Northern autumn-winter of 2005–2006. Additionally, multicolour BI photometry was also collected to study the phase shifts and amplitude ratios, between light curves obtained in different filters, for modal discrimination of the main excited modes.
Results. The detailed frequency analysis revealed a very rich and dense pulsational content consisting of 25 significant peaks, 22 of them corresponding to independent modes: one is the already known main periodicity $f_0 = 25.5765$ cd^{-1} ($\Delta V = 153$ mmag) and the other 21 are excited modes showing very small amplitudes. Some additional periodicities are probably still remaining in the residuals. This represents the most complex spectrum ever detected in a high-amplitude pulsator of this type. The majority of the secondary modes suspected from earlier works are confirmed here and, additionally, a large number of new peaks are detected. The amplitude of the main periodicity f_0 seems to be stable during decades, but the majority of the secondary modes show strong amplitude changes from one epoch to another. The suspected fundamental radial nature of the main periodicity of BL Cam is confirmed, while the secondary peak $f_1 = 25.2523$ cd^{-1} is identified as a nonradial mixed mode g_4 with $\ell = 1$. The radial double-mode nature, claimed by some authors for the main two frequencies of BL Cam, is not confirmed. Nevertheless, the frequency $f_6 = 32.6464$ cd^{-1} could correspond to the first radial overtone.

Key words. stars: variables: δ Sct – stars: individual: BL Camelopardalis – stars: oscillations – techniques: photometric

1. Introduction

High-amplitude pulsators in the Lower Classical Instability Strip (that is, δ Sct (Pop. I) and SX Phe (Pop. II) variables with full visual amplitudes larger than roughly $0\overset{\mathrm{m}}{.}3$) have been assumed for a long time to present very simple spectra with only one or two radial modes excited, mainly the first two radial modes. However, detailed studies, carried out during recent years, have shown a few exceptions to this general picture. The most remarkable one is that of the high-amplitude δ Sct star V974 Oph ($\Delta V = 0\overset{\mathrm{m}}{.}4$, Rodríguez et al. 2000) where Poretti (2003) finds five independent frequencies, with several likely nonradial modes, resembling the much more complex power spectra of the low-amplitude δ Sct variables. In a few other cases of high-amplitude pulsators, previously assumed as pure monoperiodic (DY Peg) or biperiodic (AI Vel, SX Phe or RV Ari) (Garrido & Rodríguez 1996; Walraven et al. 1992; Pócs et al. 2002), one or more additional radial and/or nonradial excited modes have been detected with very small amplitudes. Hence, these objects can be considered as very interesting targets for asteroseismological studies.

BL Cam is probably the best of these targets, at least the most complex. This is a field high-amplitude SX Phe variable ($\Delta V = 0\overset{\mathrm{m}}{.}33$, Rodríguez et al. 2000) with very low metal content ([M/H] = −2.4, McNamara 1997) where multiperiodicity has been detected in its light curves by different authors (see Fauvaud et al. 2006, for a review, hereafter F06). Besides the main periodicity, at least six additional independent modes seem to be excited in this star, the majority probably nonradial. The possibility of a radial double-mode nature for the main two periodicities has also been claimed by some authors, similar to a typical "pure" radial double-mode high-amplitude δ Sct and SX Phe-type variables. However, in this double-mode hypothesis, the true value of the secondary frequency around 31.6 cd^{-1}, or its 1 cd^{-1} alias 32.6 cd^{-1}, need to be further investigated. This determination is very important as different frequency ratios have consequences in understanding its double-mode nature in the Petersen diagrams (Poretti et al. 2005; Suárez et al. 2006).

Concerning the behaviour of the main periodicity in the (O–C) diagram, F06 found that this can be described by two terms: 1) a secular increase of the main periodicity at a rate of

Article published by EDP Sciences and available at http://www.aanda.org or http://dx.doi.org/10.1051/0004-6361:20077514

Table 1. Participating sites and instrumentation. Observatory code: AlO = Algiers Observatory, Bak = Baker Observatory, BHO = Beersel Hills Observatory, Bos = Bossmo Observatory, Cal = Calina Observatory, ChR = Château-Renard Observatory, DAO = Dominion Astrophysical Observatory, Ege = Ege University Observatory, FjO = Fjellhamar Observatory, Gil = Gilman Observatory, GOO = Groruddalen Optical Observatory, Mah = Mahill Observatory, Mar = Martin Observatory, OJP = Observatory and Planetarium of Johann Palisa, Ond = Ondrejov Observatory, OPO = Orson Pratt Observatory at Brigham Young University, PiM = Pic du Midi Observatory, SFO = Sulphur Flats Observatory, SNO = Sierra Nevada Observatory, TNO = Turkish National Observatory. Notes: a) filter *V* was used on 2 nights, but filter *B* only one night, b) filters *I* and *R* were also used on 2 and 1 nights, respectively, c) 7 nights in filter *V* and 5 using filter *R*, d) 20 nights without filter, 4 using filter *R* and one using Johnson *V* filter, e) 5 nights with a Bessel *V* filter and the last 3 ones without filter, f) filter *B* was not used during the first observing night of this run. The number of hours collected in *V*, *B* and *I* filters was 76.7, 64.0 and 72.0, respectively, g) one observing night in filter *V* and another night using both *B* and *V* filters.

Obs	Location	Longitude	Latitude	Telescope (m)	Filters	Nights	Hours	Notes
TNO	Antalya (Turkey)	30°20' E	36°49' N	1.50	*BV*	2	13.1	a
Ege	Izmir (Turkey)	27°16' E	38°25' N	0.40	*V*	1	4.6	
OJP	Ostrava (Czech Republic)	18°09' E	49°50' N	0.20	*V*	11	34.1	b
Ond	Ondrejov (Czech Republic)	14°47' E	49°55' N	0.65	*VR*	12	30.0	c
Bos	Mo i Rana (Norway)	14°07' E	66°20' N	0.20/0.25	no	25	140.2	d
FjO	Fjellhamar (Norway)	10°58' E	59°56' N	0.20	*V*	4	7.8	
GOO	Groruddalen (Norway)	10°55' E	59°57' N	0.25	no	1	1.0	
Cal	Carona (Switzerland)	8°56' E	45°47' N	0.30	no	5	17.1	
ChR	Saint-Véran (France)	6°54' E	44°42' N	0.62	*V*	11	96.7	
BHO	Beersel (Belgium)	4°18' E	50°46' N	0.40	*V*	8	24.0	e
SNO	Granada (Spain)	3°23' E	37°04' N	1.50	*BVI*	13	76.7	f
AlO	Algiers (Algeria)	3°03' E	36°47' N	0.80	*V*	1	1.9	
PiM	Pic du Midi (France)	0°09' E	42°56' N	0.60	no	4	14.4	
Mar	Blacksburg (USA)	80°33' W	37°20' N	0.40	*BV*	2	4.0	g
Gil	Gilman (USA)	87°56' W	41°27' N	0.30	*V*	2	8.4	
Bak	Springfield (USA)	93°02' W	37°24' N	0.40	*V*	7	25.8	
Mah	Mahill (USA)	105°32' W	32°54' N	0.25	*V*	2	5.7	
SFO	Jemez Springs (USA)	106°38' W	35°53' N	0.41	*V*	9	86.7	
OPO	Provo (USA)	111°39' W	40°14' N	0.40	*V*	4	8.4	
DAO	Victoria (Canada)	123°25' W	48°31' N	1.80	*V*	3	5.3	

$\mathrm{d}P/P\mathrm{d}t = 117(\pm3)\times10^{-9}$ yr^{-1} and 2) a perturbation from a companion in a binary system with a rather eccentric orbit with period of 10.5(±0.2) yr. However, discontinuous variations in the period change could not be completely discarded and a more detailed analysis is needed with the help of additional times of maxima.

For these various reasons, we undertook a follow-up campaign of BL Cam. Our main aim is to perform a detailed, long-term study concerning: 1) its pulsational content and 2) the behaviour of the main period in the (O–C) diagram. So, we carried out a multisite photometric campaign centred mainly in the period autumn-winter 2005–2006 with observations from a number of observatories in Europe and North America. These observations have been preponderantly collected in the Johnson *V* filter, in order to perform a detailed frequency analysis. Those obtained in different filters, will be used to find reliable modal discrimination for the main excited modes. The observations considered as additional (i.e. acquired using "smaller" telescopes or "without any filter") will be used to determine additional times of light maxima, in order to further improve the (O–C) analysis (Fauvaud et al. 2007). In the present work we describe the results concerning the star's pulsational content.

2. Observations

The data have been collected between August, 2005 and March, 2007 at 20 observatories in Europe and North America. Table 1 presents a summary with the list of the observatories, instrumentation and journal of the observations secured in this work. In total, photometric data have been acquired on 126 nights and 606.7 h, and most of data (i.e. 551.1 h over 108 nights) have been obtained between August, 2005 and March, 2006. All observations were obtained with CCD cameras. The majority of data were collected using the Johnson *V* filter in order to get a homogeneous data set to perform a reliable frequency analysis. The integration times, typically 20 to 120 s, have been adopted according to the instrumentation used in each case.

Additionally, some data were obtained in other filters, *BRI*, depending on the availability of each participating observatory. In particular, at Sierra Nevada Observatory (SNO), the data were acquired sequentially in filters *BVI* on 13 nights. The integration times were typically of 40, 30 and 20 s in *B*, *V* and *I* filters. Figure 1 shows one example of *BVI* light curves of BL Cam obtained during one night using the 1.5 m telescope at SNO. This figure clearly shows the differences in amplitude among different filters and the slight modulation existing along the main periodicity due to additional excited modes.

As seen in Table 1, observations without any filter and/or with some very small telescopes were also acquired. These data were used only to determine new times of light maxima. In total, about 600 new times of light maxima have been obtained in this work, very useful in order to make a detailed study on the (O–C) diagram and main periodicity behaviour of BL Cam.

In this campaign, unfortunately, there is not any data set from Asia, which could have helped to avoid the 1 cd^{-1} alias problem entirely (see Table 1). Nevertheless, the power of this alias is strongly reduced to about 56% thanks to the two continents involved, and to a good choice of the data sets for the subsequent frequency analysis.

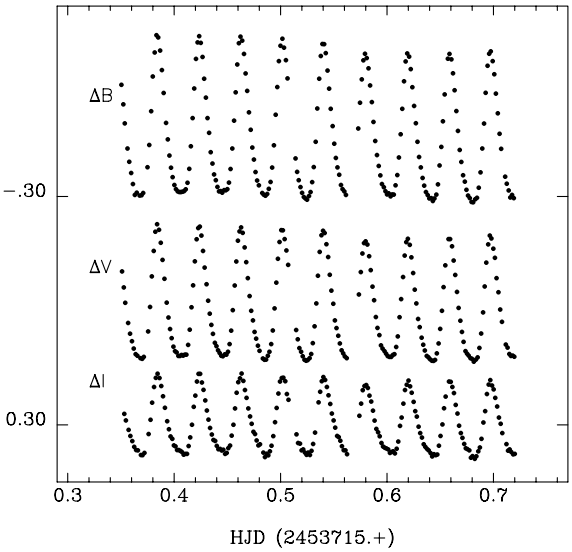

Fig. 1. *BVI* light curves of BL Cam obtained on December 10th, 2005 at Sierra Nevada Observatory.

3. Data reduction

All measurements were obtained by the method of synthetic aperture photometry. Each CCD frame was corrected for dark, bias and flat-field. After checking their stability, stars 4, 9, 12, 15, and 20 (after Fig. 1 of Hintz et al. 1997), located in the same frame as the variable, have been selected as comparison stars for BL Cam in order to derive magnitude differences. The typical photometric uncertainties, estimated from the standard deviation of the magnitude differences between comparison stars, range between $0\overset{m}{.}005$ and $0\overset{m}{.}030$, depending on each participant observatory.

In the particular case of the SNO contribution, typical uncertainties of 5, 6 and 7 mmag were derived in filters *B*, *V* and *I*, respectively, for comparison stars of similar magnitude and spectral type than BL Cam. In these frames, more than 20 stars up to about 3 mag fainter than the variable were selected for checking variability. Nevertheless, during the observations reported here, no variations have been found for any of these objects. The upper limit of non-variability depends, in each case, of the apparent magnitude of the stars: from less than one millimagnitude (for those stars of brightness similar to BL Cam) up to nearly $0\overset{m}{.}01$ for the faintest ones. In particular, stars 9 and 12 (Fig. 1 of Hintz et al. 1997), used as main comparison stars for the SNO data reduction, are found as constant above about 0.6 mmag in our region of interest (the region beyond 10 cd^{-1}). In the low frequency dominion (below about 2 cd^{-1}), this limit increases up to a few millimagnitudes probably due to observational uncertainties.

From our SNO and DAO runs, we confirm the occurrence of an adjacent faint star close to BL Cam, as previously reported in Kim et al. (2003). We estimate its magnitude to be about $V = 17\overset{m}{.}3$, and its separation to be 5.1(±0.3) arcsec from BL Cam ($V = 13\overset{m}{.}1$, Rodríguez et al. 2000), in agreement with Kim et al. (2003). However, we find a position angle around 256°, according to the definition of such position angle as given by, e.g., Green (1985). This faint star cannot be resolved under poor seeing conditions and/or small size telescopes. Thus, it was not separated in our photometric data reduction from BL Cam itself. Nevertheless, this has not any influence on our results.

Table 2. Contributions used for the frequency analysis. σ means residuals after extraction of the full solution of 25 peaks listed in Table 3. Observatory codes are the same as in Table 1.

Obs	Nights	Hours	Points	σ (mmag)
ChR	10	94.0	1435	20.8
SNO	13	76.7	1719	9.1
Bak	7	25.8	600	11.6
SFO	9	86.7	1851	9.8

4. Frequency analysis

The study of the pulsational content in BL Cam has been carried out following the procedure described in Rodríguez et al. (1998) where Fourier and least-squares algorithms are combined in the same computation program package. This method is similar to that followed by the computation package PERIOD (PERIOD04) (Lenz & Breger 2005) and both produced identical results in our analysis. When a new peak is found as significant in the frequency domain, this and all the previously determined frequencies are simultaneously optimized and extracted from the data together with the corresponding amplitudes and phases that minimize the residuals. Thus, the method does not depend on successive prewhitening of the data.

We stop the analysis when the new peaks suggested in the periodograms are not formally significant. Following Breger (1993, 1999), a peak is considered as significant when the amplitude signal/noise (S/N) ratio is larger than 4.0 for independent frequencies or 3.5 for harmonics or frequency combinations. Once all the significant peaks were removed from the periodograms, the noise level was calculated on the residuals. This was made, in a first way, by averaging the amplitudes of the residuals over 5 cd^{-1} boxes around each frequency under consideration. However, as we will comment later, a mean noise level was also determined over a much larger region of interest.

In order to make our analysis as consistent as possible, only the most reliable contributions from Table 1, with observations in the filter *V* and longest data sets, were taken into account in our frequency analysis. In this way, we chose the four sets listed in Table 2: two from Europe (ChR and SNO) and another two from America (Bak and SFO). This strongly reduces the power of the daily (1 cd^{-1}) alias from 81% (when only the SNO contribution is considered) to about 56% and allows us a better identification of the true peaks in the periodograms, as can be seen in Fig. 2. The full data set considered in Table 2 consists of 5605 measurements collected along 283.2 h of observations on 39 nights with a time span of 128 days from October, 2005 to March 2006. One night was removed from the global ChR contribution because the corresponding observing run is too short and far from the rest of the nights. The last column in Table 2 is the residual's rms in each contribution after extracting the final solution listed in Table 3. As shown, the ChR data set is much noisier than the others. Thus, this large contribution was considered with weights reduced in about 30% relative to the rest.

Before performing the frequency analysis on the full data set of Table 2, a sinusoidal variation of amplitude about $0\overset{d}{.}003$ and period about 150 days was detected in the (O–C) diagram, produced by the light-time effect in a binary or multiple system (Fauvaud et al. 2007). This effect leads to a slight shift of the main frequency, f_0, depending on the chosen data set. This is probably the cause, at least partially, why different authors find slightly different values for the main frequency f_0 of BL Cam. A clear example is shown in Table 2 of Zhou et al. (1999). Thus,

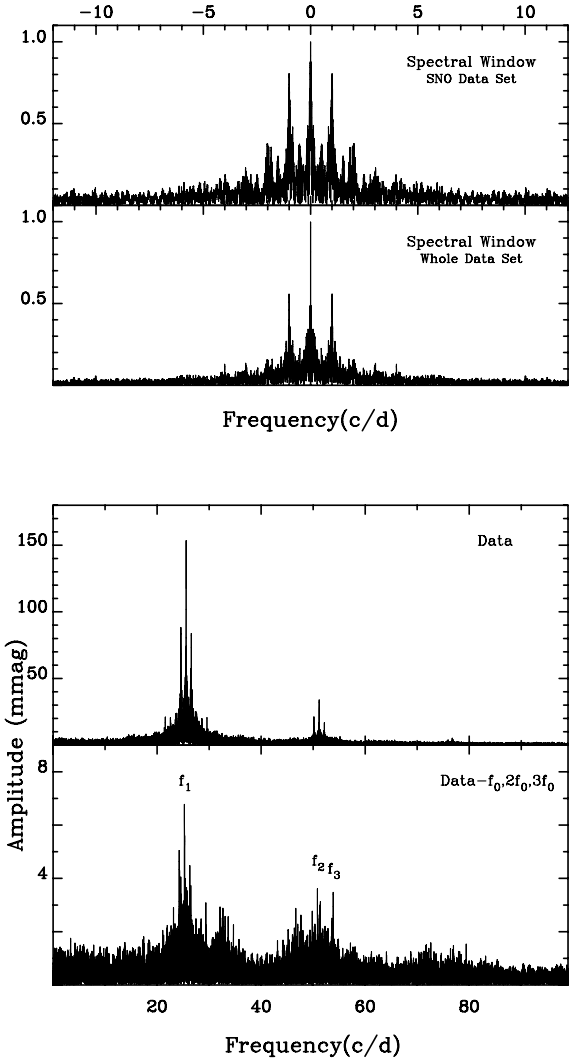

Fig. 2. *Top panels*: spectral windows of BL Cam in the filter V corresponding to the SNO and whole data sets. *Bottom panels*: amplitude spectra before and after removing the main periodicity f_0 = 25.57647 cd^{-1} together with its two harmonics $2f_0$ and $3f_0$.

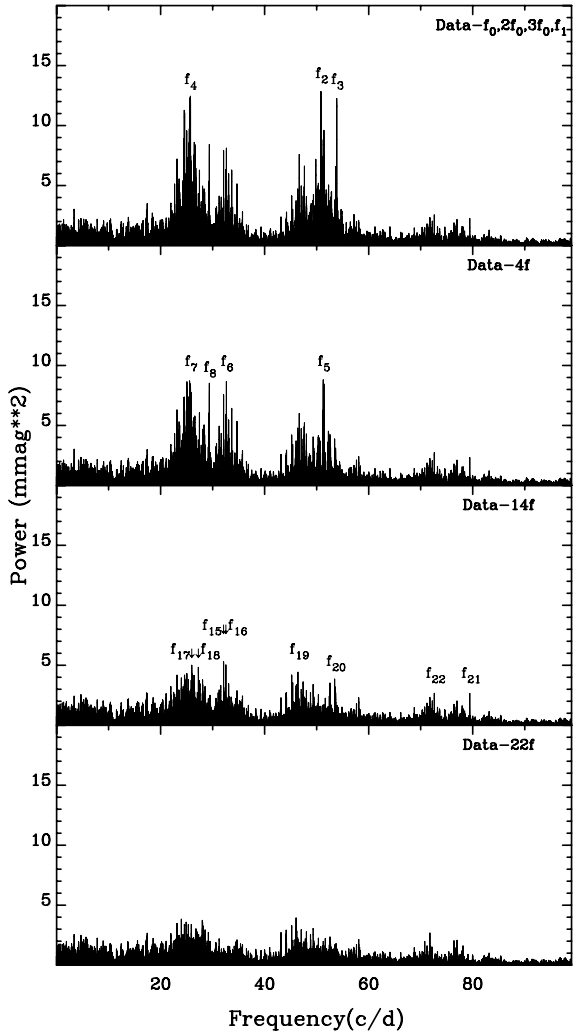

Fig. 3. Power spectra of the residuals of BL Cam after removing different sets of simultaneously optimized peaks.

we removed this effect from our data before to carry out the frequency analysis.

Moreover, each individual contribution in Table 2 was investigated to avoid misinterpretations in our final results as due to errors coming from a particular subset. This was done with the aim to obtain a final data set as homogeneous as possible. This way, inaccurate points were eliminated, and each data subset was moved to $\langle V \rangle = 0$. Next, the full amplitude of the main frequency f_0 was determined by simultaneously extracting the three significant terms f_0, $2f_0$ and $3f_0$ from each data subset and then compared with that derived from the SNO contribution. As expected, the transformation factors are very close to unity, ranging between 1.028 and 1.065, i.e. showing a good agreement between the different instrumental systems. Finally, we transformed the instrumental amplitude of each contribution to ΔV amplitudes of the SNO data set.

4.1. Results

A frequency analysis of the full data set revealed the main frequency f_0 as 25.57647(±0.00001) cd^{-1} with its first two harmonics $2f_0$ and $3f_0$ being significant. Then, the three terms were removed from the data and the residuals were analysed. The results are shown in Figs. 2 and 3 and Table 3. In a first step the periodograms show a main secondary peak f_1 = 25.25226 cd^{-1} together with f_2 = 50.82930 cd^{-1} and f_3 = 53.85668 cd^{-1}. f_1 was already detected by F06 when analysing the two data sets collected by Zhou et al. (1999, 2001), whereas f_2 corresponds to the coupling term $f_0 + f_1$.

As an additional test, the partial contributions were also checked before analysing the full data set of the residuals in order to prove that, at least, the strongest secondary peaks are intrinsic, not a consequence of artificial coupling of the data. In this sense, the periodograms were investigated in all the $0 - f_N$ range where f_N is the frequency of Nyquist. In our case, $f_N \approx 240$ cd^{-1}. However, no signal of periodicity was found in the frequency region larger than 80 cd^{-1}.

The situation was quite different in the low frequency domain, i.e. lower than about 5 cd^{-1}: a number of peaks appeared in this zone (mainly below 2 cd^{-1}) with amplitudes ranging from 5 to 2 mmag. We consider that none of them is real because in all cases they strongly depend of the data subset considered. Moreover, none of these peaks corresponds to combinations of the high frequency significant peaks. They are probably generated by systematic observational errors as instrumental drifts, residual sky transparency variations or nightly zero-point shifts

Table 3. Results from Fourier analysis with frequencies ordered in the same order as they appear in the periodograms. Sigma of residuals is 14.2 mmag. Signal/noise S/N (1) ratio means that the noise levels are determined using 5 cd^{-1} boxes around each frequency. S/N (2) means that a mean noise level of 0.49 mmag, determined from the intervals 10–20 and 30–45 cd^{-1}, has been used for peaks in the range lower than 60 cd^{-1}. Notes: a) this peak corresponds to the frequency f_2 of F06, b) $f_2 = f_0 + f_1$ and appears in F06 too, c) this peak corresponds to f_7 in F06, d) this peak corresponds to the 1 cd^{-1} alias of f_1 in F06, e) this peak corresponds to the 1 cd^{-1} alias of f_6 in F06, f) this peak corresponds to f_4 in F06.

Frequency (cd^{-1})	ΔV (mmag)	S/N (1)	S/N (2)	Notes	Frequency (cd^{-1})	ΔV (mmag)	S/N (1)	S/N (2)	Notes
	±0.29					±0.29			
f_0 = 25.57647	153.29	223.2	312.8		f_{11} = 46.64909	2.60	4.3	5.3	
$2f_0$	34.08	61.4	69.6		f_{12} = 24.54734	3.08	4.5	6.3	
$3f_0$	5.78	13.9	13.9		f_{13} = 51.39570	2.94	5.3	6.0	
f_1 = 25.25226	7.35	10.7	15.0	a	f_{14} = 51.18964	2.46	4.4	5.0	
f_2 = 50.82930	3.39	6.1	6.9	b	f_{15} = 32.10294	2.00	3.9	4.1	e
f_3 = 53.85668	4.44	9.1	9.1		f_{16} = 32.54533	2.07	4.0	4.2	f
f_4 = 25.63866	2.33	3.4	4.8	c	f_{17} = 25.99419	2.64	3.8	5.4	
f_5 = 51.25561	2.49	4.4	5.1		f_{18} = 27.26231	2.36	3.5	4.8	
f_6 = 32.64641	3.07	6.0	6.3	d	f_{19} = 46.39001	2.09	3.4	4.3	
f_7 = 25.73943	3.86	5.6	7.9		f_{20} = 53.44596	1.94	3.9	4.0	
f_8 = 29.35951	3.05	5.1	6.2		f_{21} = 79.43351	1.66	4.9	4.9	
f_9 = 25.01079	3.27	4.8	6.7		f_{22} = 72.60920	1.62	4.0	4.0	
f_{10} = 25.35245	3.48	5.0	7.1						

in data coming from different observatories. This can increase the noise at higher frequencies due to spectral leakage. For this reason, these peaks were removed from the data and, then, the remaining residuals were analysed. The results are shown in the bottom panel of Fig. 2, Fig. 3, and Table 3. In order to check our results, the resulting frequency solution was compared with that obtained without previously filtering the low-frequency peaks. The results are essentially the same.

In Table 3, the frequencies are ordered in the same order that detected in our analysis. Note that this order is not the same as that corresponding to the decreasing amplitude in the final solution, because the fit including several close frequencies produces changes in the amplitudes. This can be an indication that our solution is not perfect, but we feel that in all cases our detections are reliable, independently of the true amplitude of each peak. Examples are the frequencies f_2, f_4 and f_5 which are clearly shown in the periodograms of Figs. 2 and 3. Moreover, f_2 (=$f_0 + f_1$) and f_4 were already detected in the work of F06 (as f_3 and f_7, respectively). Hence, there is no reason to mistrust their reality.

Concerning the formal significance of the peaks, in some cases the signal/noise (S/N (1)) ratios are below the limit 4.0. This is because: a) the final amplitudes of these peaks are lower than the "original" amplitudes when they were found in the periodograms and b) in some frequency regions, the noise level is higher than the mean, probably because some periodicities are still remaining in the residuals. If we consider a mean noise level determined from a much larger interval ([10–20] and [30–45] cd^{-1}), where the noise seems to be flat, all the peaks can be considered as significant.

As shown in Table 3, some of the modes detected were already found in the work of F06. Indeed, the majority (except f_5 = 25.91 cd^{-1}) of the secondary peaks suspected in that work are confirmed in the present analysis. As summary, we find 25 significant peaks, 22 of them corresponding to independent frequencies: one is the main pulsation frequency with high amplitude and the other 21 are modes showing very small amplitudes. Some peaks could still remain in the residuals. The residual light curves of BL Cam (after extracting the main periodicity f_0 and its two harmonics $2f_0$ and $3f_0$) and Fourier fitting solution are shown in Fig. 4. The synthetic light curve fits most of the observational data, except for a few nights where the observations present higher scatter.

4.2. Discussion

4.2.1. The main frequency and amplitude variations

As in previous works, the main frequency f_0 = 25.57647(±0.00001) cd^{-1} shows as significant its first two harmonics only, $2f_0$ and $3f_0$, and seems to be stable from a pulsational point of view.

Nevertheless, as already mentioned, some variability of the main periodicity is detected from the (O–C) diagram of the light curve maxima as produced (F06) by: a) a secular term that could be due to the stellar evolution, and b) probable binarity with a time scale of several years.

Moreover, a periodic variability with time scale of about 150 days and full amplitude of about $0\overset{d}{.}003$ (probable multiplicity) is also found, from the (O–C) analysis, when we use the new data of the present multisite photometric campaign (Fauvaud et al. 2007). This can produce slightly different results for f_0 when performing a Fourier analysis. Indeed, our adopted value for f_0 is slightly different from 25.5769 cd^{-1} which corresponds to the mean period determined from the (O–C) analysis in Zhou et al. (1999). This is in agreement with the slightly different results obtained when different combinations of our data subsets are analysed. This can also be responsible for the slightly different frequencies published in the literature for the main pulsation of BL Cam. As an example, see Table 3 of Zhou et al. (1999).

Concerning the amplitude of f_0, it seems to be stable too. The value found in this work is of 153.29 mmag (Table 3) which is within the range of values determined in Table 3 of F06 and differs in about 4.7% from the mean value of 146(±10) mmag derived by those authors. Note, that the error bars in amplitude in our Table 3 are only the "formal" error bars from the Fourier fitting, as result of the multiple-frequency nonlinear least-squares fit to the data. These are in very good agreement with those error bars obtained using the analytically derived formula of Montgomery & O'Donoghue (1999). However, our V magnitudes are instrumental magnitudes, not standard ones: as discussed in previous sections, the V amplitudes determined from the different contributions in our Table 2 differ between 2.8%

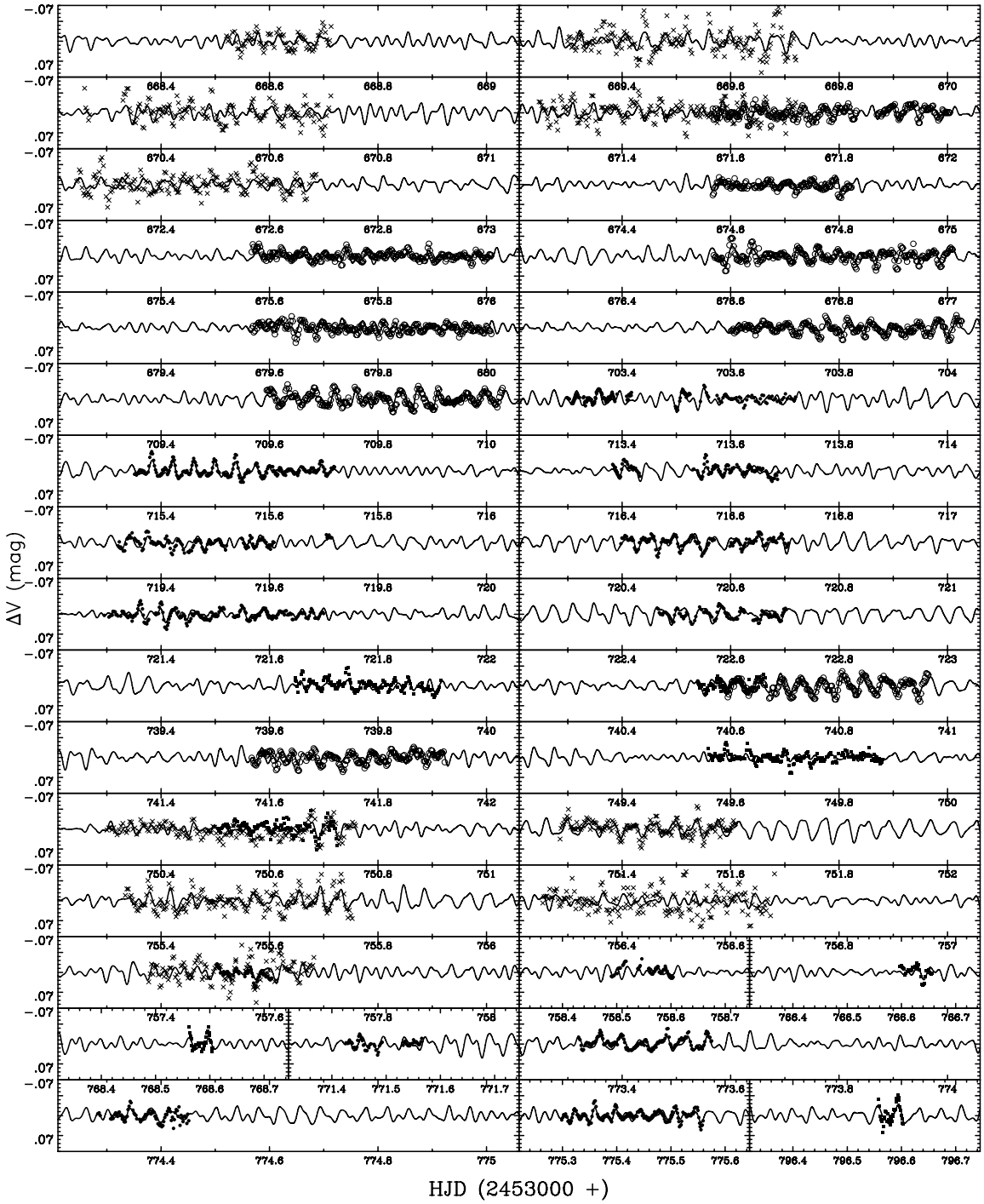

Fig. 4. Light curves of BL Cam corresponding to the residuals after removing the main periodicity and Fourier fitting using the 22-frequency solution of Table 3. The different contributions are: ChR (crosses), SNO (filled circles), Bak (filled squares) and SFO (open circles).

and 6.5% from the SNO V amplitude. Thus, we do not find a significant change in the V amplitude of the main term f_0 of BL Cam when compared to the values found in F06.

Nevertheless, concerning the amplitudes of the secondary modes, the error bars, as due to the use of instrumental magnitudes, are of the same order as the "formal" error bars in Table 3. Thus, we can say that all the secondary modes in Table 3, which were already detected in F06, present changes in amplitude.

Moreover, the small errors mentioned above have no influence in our analysis of the modal discrimination by multicolour photometry that will be carried out in Sect. 5.

4.2.2. The 31-32 cd^{-1} range

One of the aims of this work was to avoid the 1 cd^{-1} alias problem and to determine unambiguously if the secondary peak in this zone is around 31.6 or 32.6 cd^{-1} or if both are present. We also wanted to study the possible double-mode nature of this star, i.e. to see if two radial modes among the main peaks coexist.

Our analysis shows that the true peak exists only in the region around 32.65 cd^{-1}, given as f_6 in Table 3. Other two detected peaks by F06 in this region are also confirmed in our analysis as f_{15} = 32.10 and f_{16} = 32.55 cd^{-1}. Hence, detection of multiple peaks in this region is confirmed.

Table 4. Fourier fit for the main periodicity of BL Cam and the six first frequencies, f_1 to f_6, as applied to the three Johnson *BVI* filters and the data set collected at SNO. Sigmas of the residuals are 15.1 (*B*), 12.0 (*V*) and 9.1 mmag (*I*).

	B		*V*		*I*	
Frequency	*A* (mmag)	φ (rad)	*A* (mmag)	φ (rad)	*A* (mmag)	φ (rad)
	±0.56		±0.42		±0.33	
f_0	184.21	2.029	153.74	2.015	91.00	1.942
		4		3		4
$2f_0$	43.10	6.009	35.78	5.999	22.14	6.012
		15		13		16
$3f_0$	7.58	4.304	5.81	4.255	3.70	4.298
		84		82		95
f_1	8.44	1.003	6.96	1.051	4.30	1.081
		66		61		76
f_2	6.27	5.222	4.89	5.185	2.61	5.333
		90		86		126
f_3	5.30	1.686	4.78	1.867	3.30	1.876
		106		88		100
f_4	4.19	3.026	2.93	3.080	2.11	3.162
		133		143		155
f_5	2.44	5.017	2.44	4.886	1.67	5.034
		230		169		192
f_6	2.86	3.336	2.58	3.502	1.64	3.278
		194		159		193

Table 5. Observed phase shifts and amplitude ratios.

Frequency (cd^{-1})	$B-I$ (°)	$V-I$ (°)	B/I	V/I
$f_0 = 25.57647$	5.0	4.2	2.02	1.69
	0.4	0.4	1	1
$f_1 = 25.25226$	−4.4	−1.7	1.96	1.62
	8.1	7.8	20	16
$f_4 = 25.63866$	−7.8	−4.7	1.99	1.39
	16.5	17.1	41	29

On the other hand, the peak $f_6 = 32.6464$ cd^{-1} implies a period ratio of $f_0/f_6 = 0.7834$, very close to the theoretical period ratio corresponding to the first overtone/fundamental radial pulsation modes (1H/F) of 0.7843 obtained from the models computed for BL Cam in this work (Sect. 5). It suggests the first radial overtone for f_6, although the strong amplitude changes which take place in this mode, when compared with previous analyses (see F06), are not a common feature among radial pulsators. Unfortunately, our multicolour photometry cannot be used to discriminate between radial or non-radial nature for this mode because of its actual very small amplitude and, hence, too large uncertainties, as shown in Table 4.

4.2.3. The 25 cd^{-1} region

The majority of the peaks detected in the review by F06 are confirmed by our analysis. The only exception should be that named f_5 in their work (25.91 cd^{-1} in Table 6 or 25.94 cd^{-1} in Table 5). Possibly, failure of detection in our analysis is because its present amplitude is below our photometric detectability level because of the strong amplitude changes that seem to be present in the secondary modes of BL Cam. Nevertheless, this peak might correspond to our detection $f_{17} = 25.99$ cd^{-1}. On the other hand, some additional peaks have also been detected in the region close to the main frequency which were not found as significant in previous investigations. All these peaks should correspond to nonradial modes if we assume that f_0 is a radial one, as it will be confirmed in later sections.

Table 6. Main stellar parameters of the theoretical models of BL Cam.

Model	M ($M_\odot$)	$\log T_{\rm eff}$	$\log L/L_\odot$	$\log g$	α
Model 1	0.98	3.901	0.700	4.289	1.8
Model 2	0.98	3.901	0.699	4.289	1.0

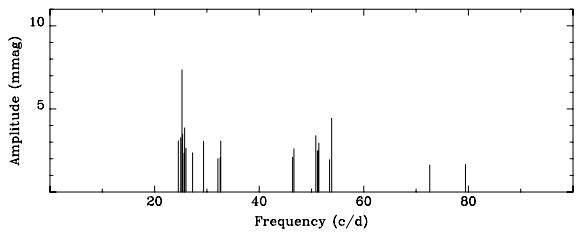

Fig. 5. Distribution of the frequencies of the detected modes. Those corresponding to the main periodicity, f_0, $2f_0$ and $3f_0$, are not shown in the figure.

Similar to F06, when analysing the best two data sets of BL Cam in the literature (those collected by Zhou et al. 1999, 2001), we also find the secondary peak $f_1 = 25.25226$ cd^{-1} as the one with the highest amplitude. However, as shown in F06, sometimes this is not true. Even, in some epochs this peak was not found as significant. A detailed look to our Table 3 and those from F06 shows that this fact is common in the secondary peaks in the 25 cd^{-1} region. All these peaks present changes in amplitude from epoch to epoch. Indeed, sometimes some of them are not detected photometrically. As commented before, strong amplitude changes have also taken place in the mode corresponding to 32.6 cd^{-1}. In fact, at some epochs this appears as the highest secondary peak.

4.2.4. Additional modes and distribution of the peaks

Figure 5 shows the frequencies detected in this work. This figure clearly shows that the detected peaks are not randomly distributed in all the frequency range, but they tend to cluster in groups as previously found in other multiperiodic δ Sct pulsators with dense spectrum of frequencies (e.g., Breger et al. 2005).

Besides the secondary peaks in the regions at 25 cd^{-1} and 32 cd^{-1}, other independent modes have been detected in BL Cam. The majority of them are grouped in well-defined zones of the spectrum: 46, 51–53 and 72–80 cd^{-1}. If we assume that f_0 is the fundamental pulsational mode p_1 (see next section), the peaks in these regions are suggested to correspond to the radial orders p_4, p_5 and p_8-p_9, respectively. Although this is the first time that these peaks have been found to be significant, the existence of some of them was already suspected in the work of F06. See, for example, the power spectrum of the residuals in Fig. 2 of that work.

One question still remains open: are there also excited modes in the low-frequency domain of the spectrum of BL Cam? The possible peaks in this region could be a consequence of the existence of additional independent modes (in such case, they should correspond to gravity modes) or the result of coupling between the already detected main modes. Unfortunately, due to the high noise present in our periodograms for this frequency region (very probably as consequence of the observational uncertainties commented in Sect. 4.1, difficult to reliably assess at millimagnitude

level in multiperiodic high-amplitude pulsators), such detection has not been actually possible.

5. Mode identification

5.1. Multicolour observations

In order to perform a modal identification of the spherical degree ℓ for the main excited modes of BL Cam, the multicolour *BVI* observations collected at SNO were used. Table 4 lists the results of the Fourier fit to the main frequencies until f_6. The results are consistent in all cases: the peaks are significant in the three filters, the amplitudes decrease as the frequency number increases, for each frequency the relative amplitudes in different filters agree with pulsations, the residuals clearly suggest the existence of additional modes.

Table 5 lists the amplitude ratios and phase shifts obtained for f_0, f_1 and f_4. A preliminary identification of the degree ℓ can be made for f_0 and f_1 by comparing this table with Fig. 2 of Balona & Evers (1999). The main periodicity f_0 corresponds obviously to a radial mode. In such case f_1 must be a non-radial mode with $\ell = 1$. Concerning f_4, although we know this must be a non-radial mode (because its frequency ratio relative to f_0 is close to unity), the error bars are too large to distinguish between $\ell = 1$ or $\ell = 2$. A more detailed study for the discrimination of these modes is presented below.

5.2. Models

We computed different theoretical models of BL Cam with the stellar evolution code CLES (Code Liegeois d'Evolution Stellaire). The global atmospheric stellar parameters of two of these models (different α values) are given in Table 6, in agreement with the parameters ($T_{\rm eff}$ = 7970 K, $\log g$ = 4.27 and [M/H] = −2.4) derived by McNamara (1997) from photometric and spectroscopic observations carried out for BL Cam. In our models, X and Z are taken as $X = 0.76$ and $Z = 0.0001$, which are typical for extreme Pop II stars similar to BL Cam. The masses and lumosities in our models are also in very good agreement with those ($M = 0.99\ M_\odot$ and $\log L/L_\odot = 0.692$) determined by McNamara (1997).

We present some evolutionary tracks obtained with the same X and Z and begining at the ZAMS (cf. Fig. 6). We see that for such low Z, masses lower than 1 $M_\odot$ are required to fit our star while crossing the instability strip during the main sequence stage. These Pop II models have no convective core, contrary to Pop I δ Sct stars. The evolution leading to SX Phe stars is still subject of controversy, and the evolution tracks given in Fig. 6 might not be representative of the real history of BL Cam. But for a given location in the HR diagram, its envelope structure is very similar to standard δ Sct stars. Hence, the driving of the modes is qualitatively the same (that is, κ-mechanism in the HeIII partial ionization zone) and the phase lags occur in same regions (H and He partial ionization sones).

The use of the non-adiabatic pulsation code MAD (Dupret 2002), fully tested for δ Sct stars, is thus entirely justified for the theoretical study of BL Cam. Time-Dependent Convection is included in our non-adiabatic models (Grigahcène et al. 2005), which leads to a much better agreement with observations, as shown by Dupret et al. (2005) for δ Sct stars. With this code we determined the normalized amplitude and phase of effective temperature variation $f_T = |\delta T_{\rm eff}/T_{\rm eff}|$ and ψ_T, for the models of Table 6 and for modes with different ℓ ($0 \le \ell \le 3$) with frequencies closest to the observed values. The values obtained for the

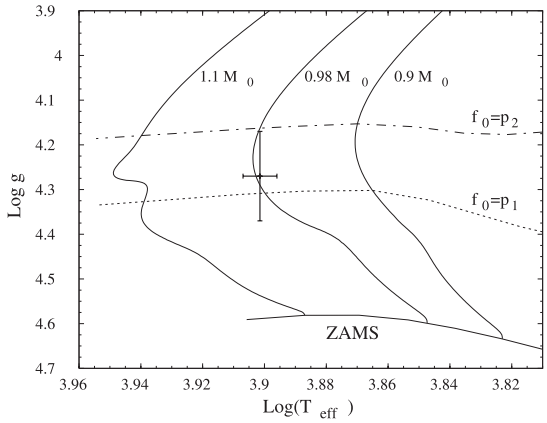

Fig. 6. $\log T_{\rm eff} - \log g$ diagram with the location of BL Cam deduced from its colour indexes (cross). Some evolutionary tracks (0.9, 0.98 and 1.1 $M_\odot$) and the location of models fitting exactly f_0 as the radial fundamental mode (dotted line) or the radial first overtone (dot-dashed line) are also shown.

fundamental radial mode are $f_T, \psi_T = (3.73, 111°)$ for model 1 and $f_T, \psi_T = (4.49, 123°)$ for model 2. The non-adiabatic results are mainly sensitive to the MLT parameter α as usually found in δ Sct stars (Moya et al. 2004). We considered models with other $T_{\rm eff}$ and $\log g$ (inside the observational error bars) and the results obtained are very similar.

Finally, taking these non-adiabatic results as input, we computed the theoretical amplitude ratios and phase differences between different photometric passbands (*I* filter taken as reference). To obtain them, we used Kurucz atmosphere models (Kurucz 1993) with [M/H] = −2.5 and [M/H] = −2.0 and the limb-darkening law of Claret (2000).

5.3. Interpretation of the frequencies

The comparison of our theoretical results with the observations is presented in Fig. 7. It is well known that amplitude ratios are more sensitive to incertitudes in the atmosphere model than phase differences for δ Scuti stars. Moreover, the phase differences give a better discrimination between different ℓ. Hence, we are more confident about the phase differences (bottom panels of Fig. 7) for the mode identifications.

As can be seen, the mode f_0 is identified as a radial mode. The best agreement is found for the model with $\alpha = 1$ (left panels, less efficient convection). Comparison with the observed frequency shows that it is probably the radial fundamental mode (see below). The error bars are larger for f_1. The best discrimination is found in the phase-difference diagram which indicates a $\ell = 1$ mode as the most probable. Comparison with observed frequency shows that it would be probably the mixed mode g_4. Finally, the error bars are too large for f_4 to allow a reliable mode identification. Because of this frequency being very close to f_0, it is certainly a non-radial mode.

The degree ℓ of the two modes f_0 and f_1 are identified. But m is unknown for f_1. At this stage only the radial mode frequency f_0 can be used to constrain without arbitrary assumption the model. In Fig. 6, the dotted line corresponds to the location of models fitting exactly f_0 as the radial fundamental mode (p_1). The dot-dashed line corresponds to models fitting f_0 as the radial first overtone (p_2). The cross corresponds to the location of BL Cam in the HR diagram as deduced from photometry with typical error bars. We see that the best solution identifies f_0 as the fundamental radial mode, although the other possibility

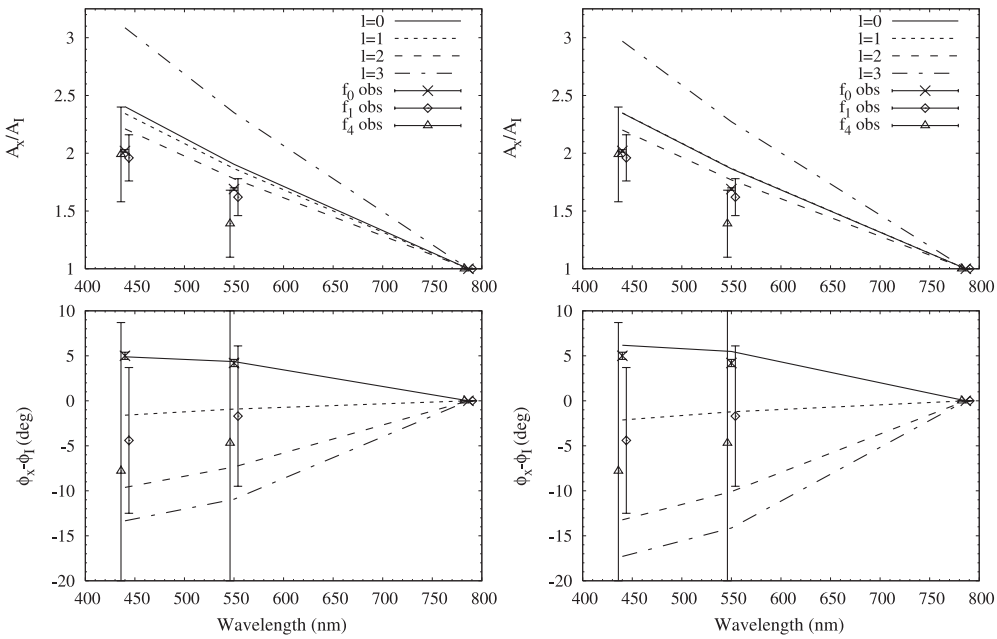

Fig. 7. Theoretical and observed B/I and V/I amplitude ratios (*top panels*) and phase differences (*bottom panels*) for a model with $\alpha = 1$ (*left panels*) and $\alpha = 1.8$ (*right panels*). The lines are the theoretical predictions for $\ell = 0$ (solid line), $\ell = 1$ (dotted line), $\ell = 2$ (dashed line) and $\ell = 3$ (dot-dashed line). The error bars correspond to the observations for f_0, f_1 and f_4.

cannot be completely discarded. For a 0.98 $M_\odot$ model, fitting exactly f_0 as the radial fundamental mode, the corresponding global parameters are $\log T_{\rm eff} = 3.900$, $\log L/L_\odot = 0.674$ and $\log g = 4.308$.

Identification of fundamental radial mode for the main frequency of BL Cam is in good agreement with that commonly derived for the main frequency in high amplitude δSct and SX Phe-type variables. This identication was already suggested for BL Cam by earlier authors on the basis of the amplitude and shape of the light curves (McNamara 1995) and the derived value of $0\overset{\rm d}{.}031$ for the pulsation constant Q.

In model 1 ($\alpha = 1.8$), the range of unstable radial modes predicted by our non-adiabatic code goes from p_1 up to p_6 (freq. ~ 60 cd^{-1}); and for model 2 ($\alpha = 1$), it goes from p_1 up to p_5 (freq. ~ 53 cd^{-1}). Hence, the excitation of all the observed modes except f_{21} and f_{22} is explained by our models.

6. Conclusions

In this work we have used the most reliable contributions of a long and extensive multisite photometric campaign to perform a detailed pulsational study of the extreme metal-deficient field high-amplitude SX Phe-type variable BL Cam. The majority of the secondary modes suspected from earlier works are confirmed here and, additionally, a large number of new peaks are detected. The results show the most complex spectrum ever detected in a high-amplitude pulsator in the Lower Cepheid Instability Strip. It consists of a large number of independent modes with very small amplitudes in addition to the already well-known main periodicity with much larger amplitude.

High-amplitude pulsators in the Lower Cepheid Instability Strip are commonly monoperiodic or double-mode radial pulsators. Only in a very few cases, some additional independent modes have been detected in their light curves which usually are non-radial (Pócs et al. 2002; Poretti 2003, and references therein). In addition to its main periodicity, the dense spectrum of independent modes with small amplitudes found in BL Cam makes this star an exotic object among the high-amplitude pulsators and a unique target for asteroseismological studies. This opens the possibility to find similar microvariability features in other classical high-amplitude objects with the use of better tools: ground-based multisite observations including observations in various passbands and/or very high-quality and homogeneous satellite data.

The radial double-mode nature claimed by some authors for the main two peaks of BL Cam (as fundamental/first overtone or first/second overtone of radial pulsation), typical in multiperiodic high-amplitude δ Sct and SX Phe-type variables, is not confirmed in this work. As regards the frequency $f_6 = 32.6464$ cd^{-1} could correspond to the first radial overtone, although it is subject to strong amplitude changes with long-term timescale which does not favour this hypothesis. Amplitude variability occurs for the majority of the secondary excited modes, but not for the main periodicity, which seems to remain stable for some decades within the observational uncertainties.

Nature of the main frequency f_0 as being a radial fundamental mode is confirmed on the basis of multicolour photometry and observed phase-shift and amplitude-ratio for different filters. This agrees well with that commonly occuring in similar high-amplitude pulsators located in the Lower Instability Strip. The secondary peak $f_1 = 25.2523$ cd^{-1} is identified as a mixed nonradial mode g_4 with $\ell = 1$.

Obviously, the full discussion given in this work is on the basis of all the peaks found as significant in our analysis are true independent peaks, corresponding to independent pulsation modes presently excited in BL Cam, with the exceptions of the harmonics $2f_0$ and $3f_0$ and the frequency combination $f_2 = f_0 + f_1$. Nevertheless, some other arguments can be presented here. It might be that some of the low-amplitude peaks close to the main frequency could be produced by amplitude and/or period variability of f_0. The presence of a clump of frequencies close to the primary peak, due to the statistical properties of the periodograms, could be indicative of the presence of a peak with a finite width, rather than a multitude of individual frequencies.

These peaks could therefore be generated by a modulation in amplitude and/or frequency of the main one rather than by multiperiodicity. Even if we accept f_1 as a real component, such a conclusion could also be applied to it. We have presented arguments that favour the hypothesis of constant amplitude of f_0 within our observational uncertainties (a few millimagnitudes). However, these uncertainties could be enough to produce the very low-amplitude secondary peaks shown close to f_0.

On the other hand, Table 3 shows some pairs of close frequencies. In particular, $f_5 - f_{14} = 0.066$ cd^{-1} and $f_4 - f_0 = 0.062$ cd^{-1}. They could indeed be separated frequency pairs or single modes with variable amplitude. The total time span of our observations is of $\Delta T = 128$ days. This means a frequency resolution of about $1.5/(\Delta T) = 0.012$ cd^{-1} (Loumos & Deeming 1978) which seems to be enough to well separate these frequency pairs. Moreover, the frequency f_4 was already detected by F06 in at least two different data sets.

Concerning the amplitude variability detected in some of the secondary peaks: it might be that some of this variability is produced by additional excited modes too close to the already detected ones to be resolved by our present data set. To gain insights on these questions, better data sets are needed based on new and extensive high-quality multisite observations.

Acknowledgements. E.G.H. acknowledges the use of the 1.8-m Plaskett Telescope at the Dominion Astrophysical Observatory, Herzberg Institute of Astrophysics, National Research Council of Canada. J.H.S. is very grateful to his group of students at the Physics Department of the Virginia Polytechnic Institute and State University. This investigation was partially supported by the Junta de Andalucía, the Spanish Dirección General de Investigación (DGI) under projects AYA2006-06375 and ESP2004-03855-C03-01, and the Grant Agency of the Czech Republic, grant No. 205/06/0217. J.C.S. acknowledges support by an I3P contract partially financed by the European Social Fund. The authors thank an anonymous referee for several valuable comments which helped to improve this paper. Acknowledgements are also made to the staff of the SNO for their help during the observations and Dr. V. Costa for proofreading. The 1.5 m telescope at SNO is operated by the Instituto de Astrofísica de Andalucía. Part of the data for this research was acquired with equipment purchased thanks to a research fund financed by the Belgian National Lottery (1999). M.H. acknowledges support by the Turkish National Observatory. This research has made use of both the Simbad database, operated at CDS, Strasbourg, France, and the Astrophysics Data System, provided by NASA, USA.

References

Balona, L. A., & Evers, E. A. 1999, MNRAS, 302, 349
Breger, M., Stich, J., Garrido, R., et al. 1993, A&A, 271, 482
Breger, M., Handler, G., Garrido, R., et al. 1999, A&A, 349, 225
Breger, M., Lenz, P., Antoci, V., et al. 2005, A&A, 435, 955
Claret, A. 2000, A&A, 363, 1081
Dupret, M.-A. 2002, Ph.D. Thesis, Bull. Soc. Roy. Sc. Liège, 5-6, 249
Dupret, M.-A., Grigahcène, A., Garrido, R., et al. 2005, MNRAS, 361, 476
Fauvaud, S., Rodríguez, E., Zhou, A.-Y., et al. 2006, A&A, 451, 999 (F06)
Fauvaud, S., et al. 2007, A&A, in preparation
Garrido, R., & Rodríguez, E. 1996, MNRAS, 281, 696
Green, R. B. 1985, Spherical Astronomy (Cambridge University Press)
Grigahcène, A., Dupret, M.-A., Gabriel, M., et al. 2005, A&A, 434, 1055
Hintz, E. G., Joner, M. D., McNamara, D. H., Nelson, K. A., & Moody, J. W. 1997, PASP, 109, 15
Kim, C., Jeon, Y. B., & Kim, S. L. 2003, PASP, 115, 755
Kurucz, R. L. 1993, ATLAS9 Stellar Atmosphere programs and 2 km s^{-1} grids. Kurucz CDROM No. 13
Lenz, P., & Breger, M. 2005, CoAst, 146, 5
Loumos, G. L., & Deeming, T. J. 1978, Ap&SS, 56, 285
McNamara, D. H. 1995, AJ, 109, 1751
McNamara, D. H. 1997, PASP, 109, 1221
Montgomery, M. H., & O'Donoghue, D. 1999, Delta Scuti Star Newsletter, 13, 28
Moya, A., Garrido, R., & Dupret, M.-A. 2004, A&A, 414, 1081
Pócs, M. D., Szeidl, B., & Viraghalmy, G. 2002, A&A, 393, 555
Poretti, E. 2003, A&A, 409, 1031
Poretti, E., Suárez, J. C., Niarchos, P. G., et al. 2005, A&A, 440, 1097
Rodríguez, E., Rolland, A., López-González, M. J., & Costa, V. 1998, A&A, 338, 905
Rodríguez, E., López-González, M. J., & López de Coca, P. 2000, A&AS, 144, 469
Suárez, J. C., Garrido, R., & Goupil, M. J. 2006, A&A, 447, 649
Walraven, T., Walraven, J., & Balona, L. A. 1992, MNRAS, 254, 59
Zhou, A.-Y., Rodríguez, E., Jiang, S. Y., Rolland, A., & Costa, V. 1999, MNRAS, 308, 631
Zhou, A.-Y., Du, B. T., Zhang, X. B., & Zhang, R. X. 2001, IBVS, 5061

[1] Instituto de Astrofísica de Andalucía, CSIC, PO Box 3004, 18080 Granada, Spain
e-mail: eloy@iaa.es
[2] Association AstroQueyras, Le Bois de Bardon, Taponnat, 16110 La Rochefoucauld, France
e-mail: stephane.fauvaud@wanadoo.fr
[3] Groupe Européen d'Observations Stellaires (GEOS), 23 Parc de Levesville, 28300 Bailleau l'Evêque, France
[4] Sulphur Flats Observatory, 449 Sulphur Creek Road, Jemez Springs, NM 87025, USA
[5] National Astronomical Observatories, Chinese Academy of Sciences, Beijing 100012 China
[6] Observatoire de la Côte d'Azur, BP 4229, 06304 Nice cedex 4, France
[7] LESIA, Observatoire de Paris-Meudon, UMR 8109, 92190 Meudon, France
[8] CRAAG, Algiers Observatory, BP 63 Bouzareah 16340, Algiers, Algeria
[9] Instituut voor Sterrenkunde, Katholieke Universiteit Leuven, Celestijnenlaan 200 B, 3001 Leuven, Belgium
[10] Variable Star Section, Norwegian Astronomical Society, PO Box 1029 Blindern, 0315 Oslo, Norway
[11] Astronomical Institute, Charles University Prague, V Holesovickach 2, 180 00 Praha 8, Czech Republic
[12] Beersel Hills Observatory, B-Beersel, Belgium
[13] Koninklijke Sterrenwacht van België, Ringlaan 3, 1180 Brussel, Belgium
[14] Ankara University, Science Faculty, Department of Astronomy and Space Sciences, 06100 Ankara, Turkey
[15] Department of Physics and Astronomy, Brigham Young University, N283 ESC, Provo, UT 84602, USA
[16] Observatory and Planetarium of Johann Palisa, VSB-Technical University, Listopadu 15, 708 33 Ostrava-Poruba, Czech Republic
[17] Martin Observatory, Physics Dep., Virginia Polytechnic Institute & State Univ., Blacksburg, VA 24061, USA
[18] Astronomical Institute, Academy of Sciences, 251 65 Ondrejov, Czech Republic
[19] Club d'Astronomie Lyon Ampère, 37 rue Paul Cazeneuve, 69008 Lyon, France
[20] Club Eclipse, 22 rue du Borrégo, Appt 5A4, 75020 Paris, France
[21] Ege University Observatory, 35100 Bornova, Izmir, Turkey
[22] American Association of Variable Star Observers, 25 Birch St., Cambridge, MA 02138, USA
[23] Akdeniz University, Art & Science Faculty, Dep. of Physics, Antalya, Turkey